Unbalanced and Reactive Load Compensation using MMCC-based SATCOMs with Third Harmonic Injection

O.J.K. Oghorada, *Member*, Li Zhang, *Senior Member*,

***Abstract*—Modular multilevel cascaded converter-based STATCOMs are scalable to higher voltages without requiring a step-up transformer with multiple windings and can be realised using a low switching frequency, giving lower harmonic content and hence a reduced filtering requirement. The paper presents a new injection technique to extend the operating ranges of MMCC STATCOMs when used for negative sequence and reactive current compensation. A non-sinusoidal voltage or current containing a fundamental and its third harmonic component is injected to achieve phase cluster voltage balance. This technique reduces the maximum dc-link voltage for the star configuration, and the maximum converter phase circulating current for the delta case, compared to applying only sinusoidal zero sequence components for mitigating the same degree of load unbalance. The analysis is confirmed experimentally, showing that the third harmonic injection can allow a significant improvement of STATCOM capability for simultaneous compensation of unbalanced load and reactive current.**

***Index Terms*—Delta, Modular Multilevel Cascaded Converter, Star, STATCOM and Unbalanced load.**

I. Introduction

VOLTAGE Source Converter (VSC)-based Static Compensators (STATCOMs) have been applied in power systems for fast dynamic reactive power compensation and voltage control. A STACOM for high power system may use multiple-winding line frequency transformers to sum the output voltages of several VSCs that have relative phase shifts between them but are not isolated at their DC supply terminals; they may in fact use only a single DC supply [1, 2]. However, the approach now is to synthesize a sinusoidal voltage from several voltage levels, typically obtained from capacitor voltage sources. Three commonly reported multilevel converters, the neutral-point-clamped (NPC), flying capacitor (FC) and cascade H-bridge multilevel converters [2, 3, 4], use capacitor voltages. They obtain more levels, hence higher voltages, by series connecting the devices without device voltage sharing problems. However, for NPC and FC types the number of the achievable voltage levels is often limited to three (or five from -v_{dc} to +v_{dc} through zero volt) not only because of voltage unbalance problems but also the voltage clamping requirement. Only the cascaded H-bridge is well suited for high-power applications because of the modular structure that enables higher voltage operation with classic low-voltage semiconductors.

In the mid-1990s a STATCOM based on cascade connection of many H-bridge converter cells with staircase modulation was presented by J Lai & Peng et al [5]. This topology has been further investigated by Marquardt et al [6], though their work was intended for HVDC applications. Since then Modular Multi-level Cascaded Converters (MMCC) have received considerable interest for STATCOM and other applications [7-12]. The modular concept offered by an MMCC makes it easily scalable to higher voltages without requiring a step-up transformer [13]. Also, it realizes a more complex output waveform using a low switching frequency, giving lower harmonic content and hence a reduced filtering requirement. Moreover, the topology is more fault tolerant, with easier manufacturing and maintenance, lower cost, higher reliability and better efficiency. The commonly accepted topology for MMCC sub-modules uses the single-phase H-bridge inverter as the basic building block [13]; a three-level flying capacitor full-bridge inverter has also been used [10]. The three phase limbs of an MMCC may be in either star or delta connection, and the whole may be classified as a Single Star Bridge Converter MMCC (SSBC-MMCC) or Single Delta Bridge Converter (SDBC-MMCC). Both have been researched for use as a STATCOM for voltage control and unbalanced load compensation [13-16].

Load unbalance is common in three-phase systems, usually due to uneven distribution of single-phase loads. Typical examples are lighting loads, single-phase traction, variable speed motor drives etc, which are all subject to large current fluctuations. Switch mode power supplies using single-phase diode rectifiers also introduce harmonic and unbalance currents. Many small renewable energy sourced generators feeding power to the distribution system exacerbates line currents imbalance. STATCOMs are effective and flexible in compensating time-varying unbalanced load currents, and examples of MMCC-based STATCOMs for this type of applications have been reported [17-19]. These are able to supply load demanded negative sequence current directly, so that the grid supplied current, and hence also the voltage at the point of common coupling, can be kept well balanced.

One of the main challenges for using the MMCC-based STATCOM is eliminating the dc-link voltage imbalance, which is caused by the stacked sub-modules in each phase having their module capacitors isolated from each other. This

produces two types of voltage imbalance: intra-phase and inter-phase imbalances. The former denotes individual module capacitor voltages in a phase cluster drifting away from their nominal levels due to unequal charging and discharging. This has been dealt with by applying suitable multilevel PWM schemes combined with closed-loop averaging dc voltage control [20, 21]. The latter, the inter-phase voltage imbalance, denotes differences in converter phase cluster voltages. This is caused by the MMCC-STATCOM supplying unbalanced power to the grid, since the isolated module capacitors prevent active power exchange between phases. Consequently dc-link voltages may drift away from their rated levels, resulting in STATCOM malfunction leading to distorted currents injected into the grid, and overstressing or even damaging the devices. The approach used for an SSBC-MMCC is to inject a sinusoidal zero-sequence voltage in the converter neutral point [17, 22-24]. For SDBC-MMCC a zero-sequence current is applied to circulate in the delta-configured three-phase limbs [19, 25]. However, such a scheme causes serious problems; in the former the injected zero-sequence voltage can cause the converter phase voltages to exceed their rated level, resulting in the SSBC operating in over-modulation mode or even becoming uncontrollable. In the SDBC-MMCC, it can lead to current being too high and exceeding the rated limit. A detailed analysis of such limitations for both the SSBC and SDBC MMCCs has been given in [25, 26], though this was for application in PV power generation. Another publication [19] highlighted the compensation limitations for a star connection STATCOM under unbalanced current compensation, and delta connection under unbalanced voltage compensation, $i.e.$ the singularity issue, without analysing the delta case for load unbalance condition. However, there is no work quantifying clearly the level of load current unbalance in relation to the phase limb voltage rating in star connection, nor to the phase current rating in delta connection. Furthermore, it is necessary to explore new method to mitigate effectively such limitations, and hence extending the MMCC-STATCOM operating ranges under unbalanced load compensation. Suggestions have been made in the context of MMCC grid-connected PV systems [25, 27-29], however the effectiveness of this approach has not been investigated, nor have the limitations been stated, particularly for MMCC-based STATCOMs.

This paper proposes a new control scheme for MMCC-based STATCOMs for unbalanced load current compensation in a power system. The method injects a non-sinusoidal voltage to a star-connected MMCC converter and a non-sinusoidal current to a delta-connected MMCC, to extend the capacitor utilization range. The injected waveform is composed of a fundamental plus its third-harmonic component. Injection of third-order harmonics in PWM controlled converters is a known technique, mostly applied to the modulation reference signals for making full use of the dc-link voltage [30, 31]. A very recent paper described work using third order injection for a grid-connected MMC-HVDC [32] and addressed the same issue as in [30, 31]; it proposed a novel curve-fitting method for evaluating the optimal magnitude and phase of the third harmonic, the objective being to minimize the modulation waveform peak values, and hence increase the capacitor voltage utilization. The work described in this current paper deals with the distinct problem of compensating the unbalanced load current. This relies on zero sequence voltage (for a star connected MMCC) and current (for a delta connected MMCC) to bring about phase limb voltage balance. The third-order injection here is intended to suppress the peak value of the zero sequence components, rather than directly dealing with the AC terminal modulation waveform. The magnitude and phase of the third-harmonic element in this application depend on the zero-sequence element which is evaluated by the three-phase power balance principle. This scheme enables effective power sharing, hence capacitor voltage balance, between phase clusters. Compared to the traditional sinusoidal zero sequence waveform injection, the technique reduces the peak phase voltages and so extends the converter operating range of an MMCC-STATCOM for unbalanced load compensation. The paper analyses and quantifies the reductions of peak phase voltage under different levels of load current imbalance and the results are compared with the conventional purely sinusoidal injection. Experimental results, obtained from a $140V$, $1.5kVA$, 2-module per phase MMCC, will be discussed and shown to validate the enhanced capabilities offered by the new control scheme.

II. Circuit Configuration of MMCC-Based STATCOMS

An MMCC-based STATCOM may be in either star (SSBC) or delta connections (SDBC) as illustrated in Figs. 1(a) and (b) respectively. For SSBC the neutral points of the supply and converter sides are not connected together. The basic cells in the phase clusters can be either two level H-bridge (2L-HB) or three level flying capacitor converter (3L-FCC). While 2L-HB generates three distinct voltage levels (0, $\pm V_{dc}$), and 3L-FCC generates five levels (0, $\pm V_{dc}$, $\pm 2V_{dc}$) respectively. Both topologies, shown in the figure below, are well-known and their applications in STATCOM devices have been reported [7, 10].

Either of these two MMCCs can be connected to the grid at the point of common coupling (PCC) for compensating the reactive power as well as negative sequence current due to unbalanced load current. However as the cells in each phase chain are isolated, the cell voltage may drift away from their rated levels when unbalanced power flows between phases, causing them giving poor performance or even malfunction. The method of using zero sequence voltage/current has been proposed for preventing such problem occurring [23], thus for SSBC-MMCC a zero sequence voltage is injected to cancel out the unbalanced power between phases and for SDBC-MMCC a zero sequence current is added. However the superimposed zero sequence elements result in the rise of SSBC-MMCC phase voltage to exceed its rated level, and current through SDBC-MMCC increases over its limit. Consequently their abilities in compensating unbalanced load current are significantly compromised.

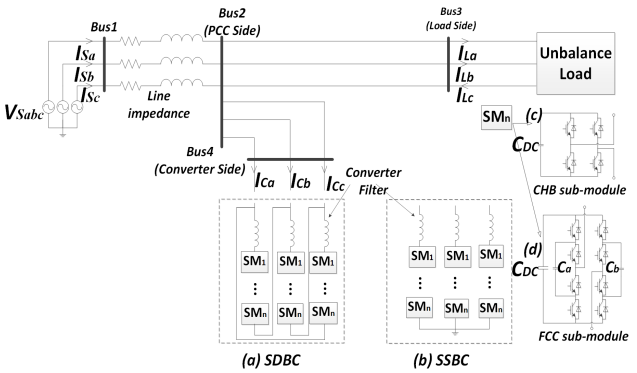

Fig. 1. Two MMCC STATCOM Systems: (a) SSBC, (b) SDBC and (c) 2L-FB, (d) 3L-FCC.

III. Phase Cluster DC-voltage Capacitor Balancing with Zero Sequence and Third Harmonic Injection

Adding third harmonic voltage components into the zero-sequence voltage in a star connected MMCC-STATCOM, or third harmonic current in its delta connected counterpart, can alleviate the problems of peak voltages or currents exceeding their limits, and so extend the phase power balancing capability in either case. A similar approach has been applied effectively in three-phase voltage source inverters for motor drive applications to extend the inverter dc-link voltage utilization [33]. The approach is analysed as follows, and its effectiveness quantified for both SSBC and SDBC cases.

A. SSBC-MMCC with Third Harmonic Voltage Injection

In this case, the voltage term injected into the phase clusters for balancing cluster powers is the sum of three: zero sequence voltage which is the fundamental element, its third harmonic component and the third harmonic of the PCC voltage expressed as:

$$v_{o_3} = \underbrace{V_o(sin(\omega t + \varphi_o)}_{v_o} + \underbrace{\frac{V_o}{6} sin(3\omega t + 3\varphi_o)}_{v_3} + \underbrace{\frac{V_p}{6} sin(3\omega t + 3\varphi_{vp})}_{v_{p3}} \tag{1}$$

The addition of 1/6 of the third harmonic components (v_3 and v_{p3}) reduces the peak cluster voltage reference to $\sqrt{3}/2$ allowing 15% increase in modulation index. Both third harmonic components are added up to the fundamental sequence component to act as the common mode component in all three clusters [25, 27].

Evaluation of all terms on the right hand side (RHS) of (1) relies on accurate estimation of the fundamental zero sequence voltage v_o, which is derived from analysing unbalanced power due to negative sequence voltage and current are described below.

1) Power Imbalance Analysis: When MMCC-STATCOM compensating unbalanced load current, the phase voltages at the PCC and the currents from the MMCC to the grid are given respectively as follows:

$$v_{sm} = V_p sin(\omega t + \varphi_{vp} - k\frac{2\pi}{3}) + V_n sin(-\omega t + \varphi_{vn} - k\frac{2\pi}{3}). \tag{2}$$

and

$$i_m = I_p sin(\omega t + \varphi_{ip} - k\frac{2\pi}{3}) + I_n sin(-\omega t + \varphi_{in} - k\frac{2\pi}{3}). \tag{3}$$

where $k = 0,\ 1,\ 2$ for $m = a, b, c$ respectively. V_p, and V_n denote positive and negative sequence voltage magnitudes, likewise I_p, and I_n for currents.

The phase power obtained by multiplying (2) and (3) contains unbalanced active powers due to the negative sequence elements in both equations, these flow through the converter phases, causing, consequently, the converter inter-cluster dc capacitor voltage imbalance.Injecting zero sequence voltage into phase cluster for canceling this power leads to converter phase voltages become:

$$\begin{aligned} v_{mM} = v_{Sm} + v_o =& V_p sin(\omega t + \varphi_{vp} - k\frac{2\pi}{3}) \\ &+ V_n sin(-\omega t + \varphi_{vn} - k\frac{2\pi}{3}) \\ &+ V_o sin(\omega t + \varphi_o). \end{aligned} \tag{4}$$

The subsequent instantaneous powers per phase cluster are evaluated according to [34] as:

$$P_m = v_{mo} i_m \quad \forall m = a, b, c, \text{ for star configuration} \tag{5}$$

and the average phase power is obtained by multiplying (3) and (4) and result taking time averaging, as given by:

$$\begin{aligned} P_m = \frac{1}{2}[& \underbrace{V_p I_p cos(\varphi_{vp} - \varphi_{ip}) + V_n I_n cos(\varphi_{vn} - \varphi_{in})}_{P_{Cm}^{++} and P_{Cm}^{--}} \\ & \underbrace{+q\frac{1}{2} V_p I_n cos(\varphi_{vp} + \varphi_{in}) + r\frac{\sqrt{3}}{2} V_p I_n sin(\varphi_{vp} + \varphi_{in})}_{P_{Cm}^{+-}} \\ & \underbrace{+q\frac{1}{2} V_n I_p cos(\varphi_{vn} + \varphi_{ip}) + r\frac{\sqrt{3}}{2} V_n I_p sin(\varphi_{vn} + \varphi_{ip})}_{P_{Cm}^{-+}} \\ & \underbrace{-q\frac{1}{2} V_o I_p cos(\varphi_o - \varphi_{ip}) - r\frac{\sqrt{3}}{2} V_o I_p sin(\varphi_o - \varphi_{ip})}_{P_{Cm}^{o+}} \\ & \underbrace{+q\frac{1}{2} V_o I_n cos(\varphi_o + \varphi_{in}) - r\frac{\sqrt{3}}{2} V_o I_n sin(\varphi_o + \varphi_{in})]}_{P_{Cm}^{o-}} \end{aligned} \tag{6}$$

where, $q = -2, 1, 1$ and $r = 0, +1, -1\ \forall m = a, b, c$.

The first two terms on the RHS in (6) are the products of positive sequence voltage and current (i.e. P_{Cm}^{++}), and negative sequence voltage and current (i.e. P_{Cm}^{--}),these are supplied by the grid to compensate for power losses across the converter. The remaining eight terms can be grouped into two sets; the first four are the cross products of both positive sequence voltage and negative sequence current (i.e. P_{Cm}^{+-}),and negative voltage and positive sequence current (i.e. P_{Cm}^{-+}).The second set is due to zero sequence voltage; which is the products of zero sequence voltage and positive or negative sequence currents (i.e. P_{Cm}^{o+} and P_{Cm}^{o-}).They can be simplified as:

$$P_{Cm} = \frac{1}{2}(P_{Cm}^{+-} + P_{Cm}^{-+} + P_{Cm}^{o+} + P_{Cm}^{o-}) \tag{7}$$

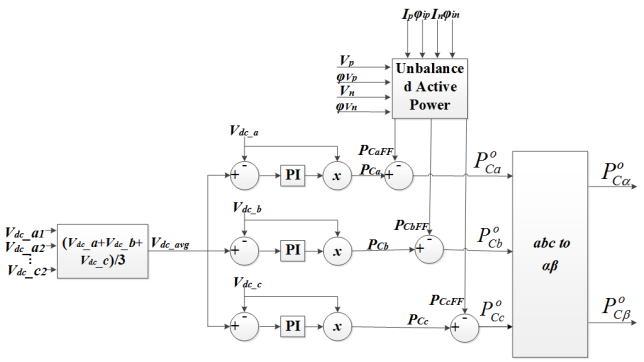

Fig. 2. Diagram of cluster voltage balancing control.

The key to preventing cluster dc voltage drifting is to maintain P_{Cm} to be zero, this requires determining the single unknown zero sequence voltage v_o.

2) Derivation of Zero Sequence Voltage and its third harmonic: A new method for estimating zero sequence voltage is proposed here as shown in Fig. 2 which will be shown giving more accurate result. In this not only does active powers, P^{-+}_{Cm} and P^{+-}_{Cm} obtained via real-time measurement, are used for feed-forward control, combining with three PI regulators for each phase limb dc voltage control, it also applies the unbalanced voltages and converter reference currents. The differences of the feed-forward from the feedback terms give per phase zero sequence average active power (P^{o-}_{Cm}) as:

$$P^o_{Cm} = \underbrace{P_{Cm}}_{P_{CmFB}} - \underbrace{(P^{+-}_{Cm} - P^{-+}_{Cm})}_{P_{CmFF}} \forall m = a, b, c \in \text{star} \tag{8}$$

The three phase active power is then transformed into α-β form relating to zero sequence voltage, thus:

$$\begin{aligned}\begin{bmatrix} P^o_{C\alpha} \\ P^o_{C\beta} \end{bmatrix} &= \frac{2}{3}\begin{bmatrix} 1 & -\frac{1}{2} & \frac{1}{2} \\ 0 & -\frac{\sqrt{3}}{2} & \frac{\sqrt{3}}{2} \end{bmatrix}\begin{bmatrix} P^o_{Ca} \\ P^o_{Cb} \\ P^o_{Cc} \end{bmatrix} \\ &= \frac{1}{2}\begin{bmatrix} A_{11} & A_{12} \\ A_{21} & A_{22} \end{bmatrix}\begin{bmatrix} V_o cos\varphi_o \\ V_o sin\varphi_o \end{bmatrix}\end{aligned} \tag{9}$$

where;

$$\begin{aligned} A_{11} &= I_p cos\varphi_{ip} - I_n cos\varphi_{in} \\ A_{12} &= I_p sin\varphi_{ip} + I_n sin\varphi_{in} \\ A_{21} &= -I_p sin\varphi_{ip} + I_n sin\varphi_{in} \\ A_{22} &= I_p cos\varphi_{ip} + I_n cos\varphi_{in} \end{aligned} \tag{10}$$

The zero sequence voltage can then be expressed as:

$$\begin{bmatrix} V_o cos\varphi_o \\ V_o sin\varphi_o \end{bmatrix} = \frac{2}{I_p^2 - I_n^2}\begin{bmatrix} A_{22} & -A_{12} \\ -A_{21} & A_{11} \end{bmatrix}\begin{bmatrix} P^o_{c\alpha} \\ P^o_{c\beta} \end{bmatrix} \tag{11}$$

where the magnitude and phase angle of the zero sequence voltage and current are given as:

$$\begin{aligned} V_o &= \sqrt{(V_o cos\varphi_o)^2 + (V_o sin\varphi_o)^2} \\ \varphi_o &= arctan\left(\frac{V_o sin\varphi_o}{V_o cos\varphi_o}\right). \end{aligned} \tag{12}$$

Subsequently its third harmonic element is:

$$V_3 = \frac{1}{6}\sqrt{(V_o cos\varphi_o)^2 + (V_o sin\varphi_o)^2} sin(3\omega t + 3\varphi_o). \tag{13}$$

It can be seen from (11) that for the SSBC-MMCC, the zero sequence voltage becomes infinite ($i.e.$ I_p=I_n), consequently resulting in one or two converter phase voltages requiring unlimitedly high cluster dc-link voltage which is not realisable. Thus the capability of a SSBC-MMCC STATCOM for unbalanced load compensation is limited by the rating of its phase cluster voltages.

B. SDBC-MMCC with Third Harmonic Current Injection

For SDBC-MMCC the injected current term is given as:

$$i_{o_3} = I_o(sin(\omega t + \varphi_o) + \frac{1}{6}sin(3\omega t + 3\varphi_o)). \tag{14}$$

1) Power Imbalance Analysis: To evaluate just injecting zero sequence circulating current, the phase cluster voltages, the converter reference currents are given respectively as follows:

$$\begin{aligned} v_m = \sqrt{3}[&V_p sin(\omega t + \varphi_{vp} - k\frac{2\pi}{3} + \frac{\pi}{6}) \\ &+ V_n sin(-\omega t + \varphi_{vn} - k\frac{2\pi}{3} + \frac{\pi}{6})]. \end{aligned} \tag{15}$$

and

$$\begin{aligned} i_{mo} = i_m + i_o = &\frac{1}{\sqrt{3}}[I_p sin(\omega t + \varphi_{ip} - k\frac{2\pi}{3} + \frac{\pi}{6}) \\ &+ I_n sin(-\omega t + \varphi_{in} - k\frac{2\pi}{3} + \frac{\pi}{6})] \\ &+ I_o sin(\omega t + \varphi_o). \end{aligned} \tag{16}$$

where φ_{ip}, φ_{in} are respectively the phase angles of the positive and negative sequence currents, and $k = 0, 1, 2$ and for $m = ab, bc, ca$ (delta) respectively.

Multiplying v_m and i_{mo} gives the equation for instantaneous power per phase cluster which are the same as (6) and (7) except phase index $m = ab, bc, ca$. Note that the last two terms in (7), P^{o+}_{Cm} and P^{o-}_{Cm} , are now due to zero sequence current multiplying respectively positive or negative sequence voltages. Similar to star connection case, preventing cluster dc voltage drifting is to maintain P_{Cm} to be zero, by using the single zero sequence current i_o circulating in the converter clusters.

2) Derivation of Zero Sequence Current and its third harmonic: This follows the same principle as that used in the SSBC case, hence the control block diagram shown in Fig. 2 is applicable here. The per phase zero sequence average active power (P^o_{Cm}) can also be evaluated by the differences between the feed-forward and feedback powers given by (8) and by applying α-β transformation, it can be expressed as:

$$\begin{aligned}\begin{bmatrix} P^o_{C\alpha} \\ P^o_{C\beta} \end{bmatrix} &= \frac{2}{3}\begin{bmatrix} 1 & -\frac{1}{2} & \frac{1}{2} \\ 0 & -\frac{\sqrt{3}}{2} & \frac{\sqrt{3}}{2} \end{bmatrix}\begin{bmatrix} P^o_{Cab} \\ P^o_{Cbc} \\ P^o_{Cca} \end{bmatrix} \\ &= \frac{\sqrt{3}}{4}\begin{bmatrix} B_{11} & B_{12} \\ B_{21} & B_{22} \end{bmatrix}\begin{bmatrix} I_o cos\varphi_o \\ I_o sin\varphi_o \end{bmatrix}\end{aligned} \tag{17}$$

where;

$$\begin{aligned} B_{11} &= \sqrt{3}(V_p cos\varphi_{vp} - V_n cos\varphi_{vn}) - (V_p sin\varphi_{vp} - V_n sin\varphi_{vn}) \\ B_{12} &= (V_p cos\varphi_{vp} + V_n cos\varphi_{vn}) + \sqrt{3}(V_p sin\varphi_{vp} + V_n sin\varphi_{vn}) \\ B_{21} &= (-V_p cos\varphi_{vp} + V_n cos\varphi_{vn}) - \sqrt{3}(V_p sin\varphi_{vp} - V_n sin\varphi_{vn}) \\ B_{22} &= \sqrt{3}(V_p cos\varphi_{vp} + V_n cos\varphi_{vn}) - (V_p sin\varphi_{vp} + V_n sin\varphi_{vn}) \end{aligned} \tag{18}$$

Hence the zero sequence current can then be written as:

$$\begin{bmatrix} I_o cos\varphi_o \\ I_o sin\varphi_o \end{bmatrix} = \frac{2}{\sqrt{3}(V_p^2 - V_n^2)} \begin{bmatrix} B_{22} & -B_{12} \\ -B_{21} & B_{11} \end{bmatrix} \begin{bmatrix} P_{c\alpha}^o \\ P_{c\beta}^o \end{bmatrix} \quad (19)$$

where the magnitude and phase angle of the zero sequence current is given as:

$$\begin{aligned} I_o &= \sqrt{(I_o cos\varphi_o)^2 + (I_o sin\varphi_o)^2} \\ \varphi_o &= arctan\left(\frac{I_o sin\varphi_o}{I_o cos\varphi_o}\right). \end{aligned} \quad (20)$$

As can be observed in (19), the zero sequence current circulating between the phases increases with the magnitude of I_p and I_n, but does not tend to infinity when I_p=I_n.

C. Evaluation of Zero Sequence Components

The magnitudes of the zero sequence components vary not only with the I_n magnitude, but also on its phase relative to V_p. To evaluate this dependence the power losses in the converters will be neglected; and the phase angle of I_P relative to V_p is $+\frac{\pi}{2}$ due to reactive power compensation. The expressions for the zero sequence voltage magnitude and phase angle are:

$$V_o = \frac{V_p I_n}{I_p^2 - I_n^2}\sqrt{I_p^2 + I_n^2 + 2I_p I_n cos(\varphi_{ip} + 3\varphi_{in})} \quad (21)$$

$$\varphi_o = arctan\left(\frac{I_p sin(\varphi_{ip} + \varphi_{in}) - I_n sin(2\varphi_{in})}{I_p cos(\varphi_{ip} + \varphi_{in}) + I_n cos(2\varphi_{in})}\right) \quad (22)$$

It can be seen from (21) that the magnitude of the zero sequence voltage depends on the magnitude and phase angles of both positive and negative sequence currents to be compensated. Two examples are used to examine the implications of this.

case1:I_p =1pu, I_n =0.5pu, the positive and negative sequence compensated currents are in phase (i.e. φ_{ip}=φ_{in}= $+\frac{\pi}{2}$), and V_p= 1pu. Then:

$$\begin{aligned} V_o &= \frac{0.5}{1^2 - 0.5^2}\sqrt{1^2 + 0.5^2 + cos(2\pi)} = \frac{0.5}{0.75}\sqrt{2.25} = 1pu \\ \varphi_o &= arctan\left(\frac{sin(\pi) - 0.5sin(\pi)}{cos(\pi) + 0.5cos(\pi)}\right) = arctan(\frac{0}{-1.5}) = 180^0. \end{aligned} \quad (23)$$

case2:I_p =1pu, I_n =0.5pu, the positive and negative sequence compensated current phase angles are anti-phased to each other (i.e. φ_{ip}=$\frac{\pi}{2}$, φ_{in}= $-\frac{\pi}{2}$), and V_p= 1pu. Then:

$$\begin{aligned} V_o &= \frac{0.5}{1^2 - 0.5^2}\sqrt{1^2 + 0.5^2 + cos(-\pi)} = \frac{0.5}{0.75}\sqrt{0.25} = 0.33pu \\ \varphi_o &= arctan\left(\frac{sin(0) - 0.5sin(-\pi)}{cos(0) + 0.5cos(-\pi)}\right) = arctan(\frac{0}{0.5}) = 0^0. \end{aligned} \quad (24)$$

These examples confirm that the phase angles of I_p and I_n influence the V_o magnitude. The 3-D plot in Fig.3 shows the general relationship of V_o with respect to both φ_{in} and I_n/I_p and further validates the above analysis. The diagram shows that the maximum V_o value not only occurs at φ_{in}=$\frac{\pi}{2}$ but also at φ_{in}=$-\frac{\pi}{6}$ and $-\frac{2\pi}{3}$, and the minimum occurs at at φ_{in} = $-\frac{\pi}{2}$, $\frac{\pi}{6}$ and $\frac{2\pi}{3}$.

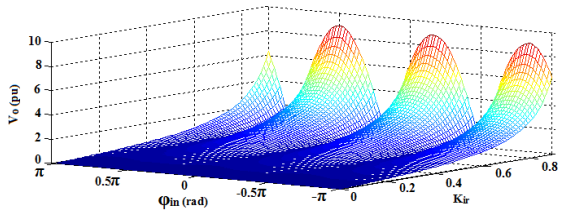

Fig. 3. Relationship between the zero sequence voltage magnitude V_o, degree of unbalance K_{ir}= I_n/I_p, and the phase angle of the negative sequence current φ_{in} at maximum PCC voltage of $230V$.

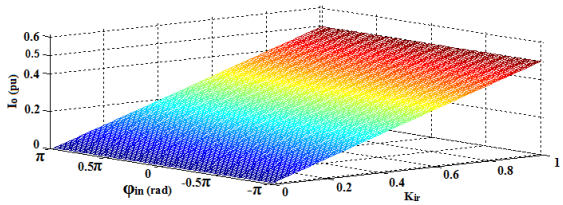

Fig. 4. Relationship between the zero sequence current magnitude I_o, degree of unbalance K_{ir}= I_n/I_p, and the phase angle of the negative sequence current φ_{in} at maximum cluster current $(2/\sqrt{3})A$.

For the SDBC, the zero sequence current is simplified as:

$$\begin{aligned} I_o &= \frac{I_n}{\sqrt{3}} \\ \varphi_o &= arctan(-cot\varphi_{in}) = 90^0 + \varphi_{in} \end{aligned} \quad (25)$$

These show the magnitude of the zero sequence current I_o is simply proportional to I_n and independent of its relative phase (see Fig. 4). It is worth noting that this differs from the case analysed in [19] which was for unbalance voltage condition (i.e.V_p=V_n).

D. Reductions of Peak Fundamental Components with Third Harmonic Injection

Evaluations of zero sequence components above lead to straightforward quantifications of the third harmonic components. Fig. 5(a) shows the waveforms of injected zero sequence voltage and the resultant converter phase cluster reference voltages when the ratio of negative to positive sequence currents, defined as k_{ir}=I_n/I_p, is set to 0.3 and they are in phase. It can be seen clearly that the magnitudes of the three phase cluster voltages are different and the peak phase voltage is $1.3pu$. Adding the third harmonic, the peak phase voltage is reduced which is shown in Fig. 5(b). The maximum phase voltage corresponding to the third harmonic injection is only $1.2pu$, which is about 8.3% lower than the zero sequence case. This reduction allows the STATCOM to compensate a higher level of current unbalance compared to when only sinusoidal zero sequence voltage is injected. In the SDBC case the current waveforms are derived for when $K_{ir} = 0.55$. The maximum phase current magnitude for the combined zero sequence current and its third harmonic is only 88% of that when only zero sequence current is injected as shown in Fig. 6. This means that for compensating the same level of load imbalance, the new harmonic current injection scheme leads to the magnitude of circulating current in SDBC phase clusters

This article has been accepted for publication in a future issue of this journal, but has not been fully edited. Content may change prior to final publication. Citation information: DOI 10.1109/TIE.2018.2849962, IEEE Transactions on Industrial Electronics

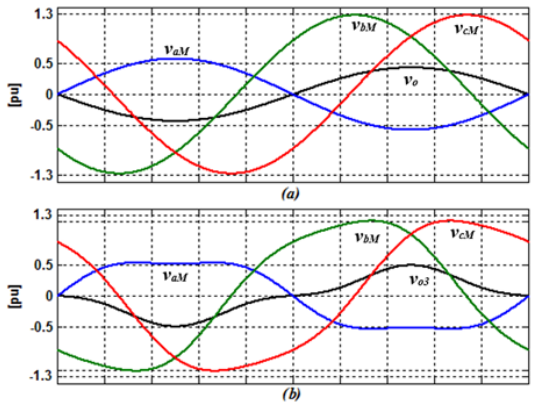

Fig. 5. SSBC converter cluster voltage waveforms (a) injecting zero sequence voltage, (b) zero sequence voltage + its third harmonic component for I_n/I_p=0.3pu.

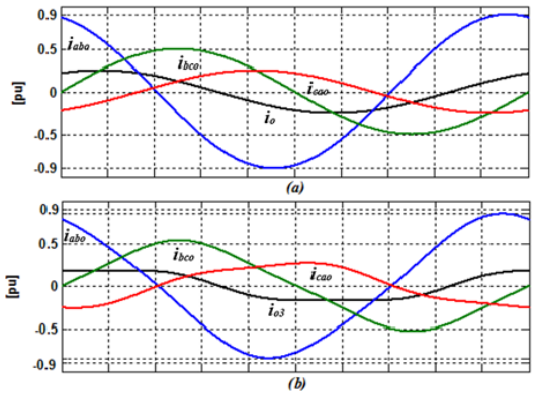

Fig. 6. SDBC converter cluster current waveforms (a) injecting zero sequence current and (b) zero sequence current + its third harmonic component for I_n/I_p=0.55pu.

significantly lower than that when using the only sinusoidal zero sequence current.

E. The Control Scheme

Fig. 7 shows the control structure of the STATCOM, which applies to either a star or a delta configured MMCC for unbalanced load compensation. This comprises four sections as shown: the extraction unit, overall dc voltage control, inter-cluster dc voltage balancing control, and current control plus PWM unit. The extraction unit as shown in Fig. 8 is used in extracting the positive and negative sequence components of the grid voltage and load currents for synchronization and also reference current generation for the current control loop. The overall dc capacitor voltage control is used in to generate the necessary positive sequence d-component current I_d^{*+} for maintaining the average dc capacitor voltages at their desired values to compensate. The inter-cluster voltage balancing control is required to maintain equality of the three phase cluster voltages. The α-β active cluster power derived from the output of the cluster balancing control loop shown in Fig. 2 is fed to determine the zero sequence components ($i.e.$ either fundamental or third harmonic components) depending on the MMCC configuration. For inter-cluster voltage balancing control of SDBC MMCC, the zero sequence current components from Fig. 2 are compared with the measured average current (i_{Cab} +i_{Cbc} +i_{Cca})/3, and the errors multiplied by a proportional gain K_{pio} are converted into voltage commands. The output signals from this part are combined with the reference voltages generated from the current control loop, hence becoming the reference signals for the PWM unit. For synthesising gate signals for controlling the converter switches the phase-shifted PWM scheme is used [35].

IV. QUANTIFICATION OF OPERATING RANGE EXTENSION

It was shown in Section III(D) that by injecting combined zero sequence voltage or current and its respective third harmonic component for unbalanced load compensation, the peak phase voltage (for star) and current (for delta) are significantly lower than when using zero sequence components only, and hence the range of unbalanced current compensation is extended. However the results in Section III(D) are only for one particular case of load unbalance, the analysis below evaluates the peak zero sequence voltage injected for SSBC case, and current for SDBC for both fundamental and third harmonic injection techniques, while the degree of load current unbalance varies from 0 to 100%, (i.e. K_{ir} from 0 to 1). The required maximum phase cluster dc-link voltage and cluster current for both star and delta case respectively can be evaluated and compared, and the more effective method should ideally give lower voltage/current ratings.

A. SSBC MMCC

In determining the phase cluster dc-capacitor voltage required by the SSBC-MMCC for load unbalance compensation, the voltages of each phase are dependent on the their cluster individual module dc-link voltages V_{dc}, and their total value $\Sigma V_{dc} = n_{mp}.V_{dc}$, where n_{mp} is the number of modules per phase. The three phase voltages may be different and the peak values of the maximum phase voltages can be defined as:

$$V_{dcrated} = Max(|V_{mM}|) \leq n_{mp}V_{dc} \tag{26}$$

where the converter output voltage is given as:

$$V_{mM} = v_m + v_o + \underbrace{L\frac{di_m}{dt} + Ri_m}_{V_f} = V_{mM}sin(\omega t + \phi_m) \tag{27}$$

and V_f defines the voltage drop across the MMCC filter; $m = a, b, c$.

Fig. 9 shows a logarithmic plot of the $V_{dcrated}$ varying according to K_{ir}, when injecting both zero sequence voltage fundamental plus the third harmonic component. It is seen that by injecting v_{o3} for inter cluster voltage balancing, the maximum cluster dc-link voltage, $V_{dcrated}$, is clearly lower than when injecting only v_o for $0 \leq K_{ir} \leq 0.45$ and $0.55 \leq K_{ir} \leq 0.9$. Within the range $0.45 \leq K_{ir} \leq 0.55$ a dead zone exists, meaning that the $V_{dcrated}$ values of both v_o and v_{o3} injection techniques are almost equal. This results from the fact that within $0.45 \leq K_{ir} \leq 0.55$ both v_o and v_{o3} are almost equal as illustrated in Fig. 9, but this only occurs for the worst

This article has been accepted for publication in a future issue of this journal, but has not been fully edited. Content may change prior to final publication. Citation information: DOI 10.1109/TIE.2018.2849962, IEEE Transactions on Industrial Electronics

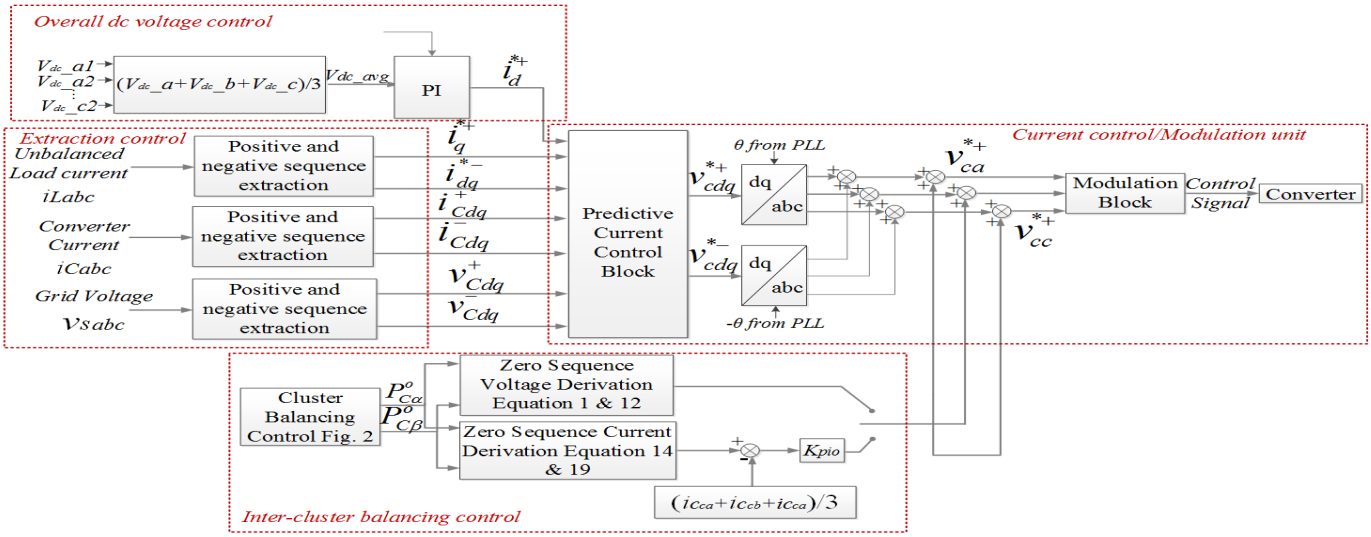

Fig. 7. MMCC based STATCOM control system.

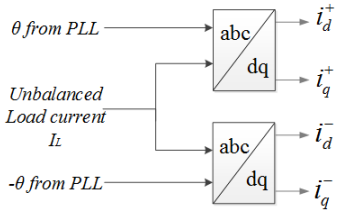

Fig. 8. Positive and negative sequence extraction.

condition $i.e.$ when φ_{ip}=φ_{in}. Thus the v_{o3} technique requires lower voltage compared to the v_o counterpart. For example, for $K_{ir} = 0.2$, the normalized peak $V_{dcrated}/V_p$ under v_o injection is about $1.18pu$ whereas for v_{o3} it is only $1.07pu$. This implies that for an 11kV distribution system compensating $K_{ir} = 0.2$ of load unbalance where each converter module is rated 400V, 33 modules would be required for both v_o injection technique, whereas with v_{o3} injection only 30 modules are required. It is therefore seen that the use of the zero sequence voltage plus its third harmonic reduces the footprint size and cost of the SSBC-STATCOM. The difference in the estimated dc-link voltage between both injection techniques is clearly shown in Fig. 10 except in the region between $0.45 \leq K_{ir} \leq 0.55$ when both techniques are equal.

B. SDBC MMCC

Comparing the current magnitudes when injecting i_o and i_{o3} as a function of K_{ir} , the one under i_{o3} is lower than that when injecting its fundamental frequency counterpart as K_{ir} varies from 0 to 1 as seen in Fig. 11.

The phase cluster currents in the SDBC are expressed as:

$$i_m = i_{mp} + i_{mn} + i_o where m = ab, bc, ca \qquad (28)$$

The current rating I_{rated} of the SDBC is determined by the maximum phase current given as:

$$I_{rated} = Max(|I_m|) \qquad (29)$$

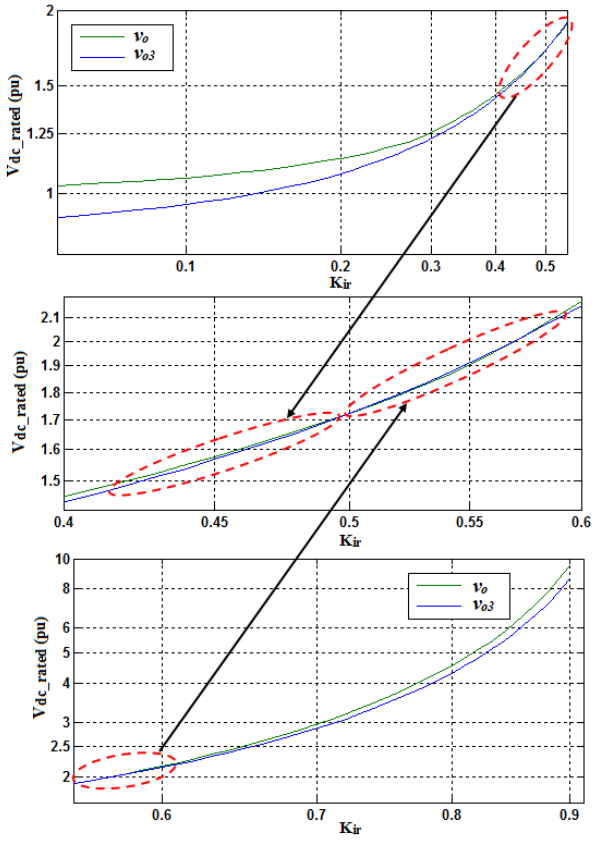

Fig. 9. Comparison between sinusoidal and third harmonic zero sequence injection with respect to estimated DC-link cluster voltage.

The maximum phase current of the SDBC only occurs when the zero sequence current is in phase with any of the phase cluster currents. Based on (28), this occurs at $\varphi_{in} = -\frac{\pi}{3}, -\pi$ and $+\frac{\pi}{3}$.

Fig. 12, shows the relationship between the maximum cluster current and the degree of unbalance K_{ir} for both the i_o and i_{o3} injections at $\varphi_{in} = -\frac{\pi}{3}$. It is seen that by injecting i_{o3}

This article has been accepted for publication in a future issue of this journal, but has not been fully edited. Content may change prior to final publication. Citation information: DOI 10.1109/TIE.2018.2849962, IEEE Transactions on Industrial Electronics

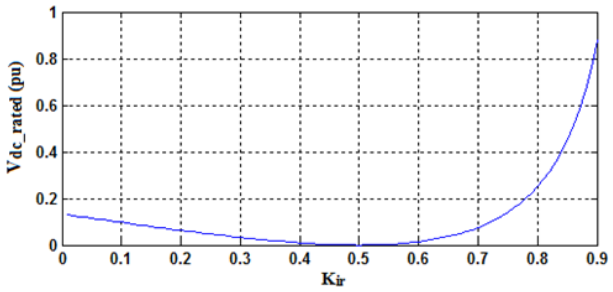

Fig. 10. dc link Voltage difference between zero sequence voltage fundamental and third harmonic injections with respect to K_{ir}.

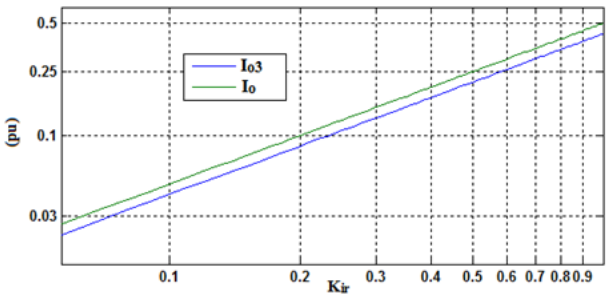

Fig. 11. Comparison between sinusoidal and third harmonic zero sequence current injection with respect to K_{ir}.

TABLE I
EXPERIMENTAL CIRCUIT PARAMETERS

Symbol	Quantity	Value
V_s	PCC Max. phase voltage	$60V$
f	Line frequency	$50Hz$
n_{mp}	Modules per cluster	2
V_{dc}	Module voltage ($400V$)	SSBC Utilized @ $50V$ SDBC Utilized @ $70V$
L_{ac}, R_{ac}	AC filter	$1mH, 1\Omega$
C_{dc}	Module Capacitor	$1120\mu F$
C_{fc}	Flying Capacitor	$560\mu F$
f_c	Carrier frequency	$750Hz$
S	Rated Power	$1.5KVA$
T_s	Sampling time	$0.1msec$

for inter cluster voltage balancing, the required cluster current rating, I_{rated}, is lower than when injecting just a fundamental component of the zero sequence current i_o. For example when $K_{ir} = 1$ the rated cluster current required for both i_o and i_{o3} injection techniques are $1.39pu$ and $1.29pu$ respectively, about 8% lower.

V. EXPERIMENTAL RESULTS AND DISCUSSIONS

The theoretical analysis presented above has been verified by experimental tests for both star and delta configurations. The experimental MMCC prototype built at the University of Leeds laboratory is shown in Fig. 13. Each of the three phase clusters of the MMCC consists of two series connected modules which are three-level full-bridge flying capacitor

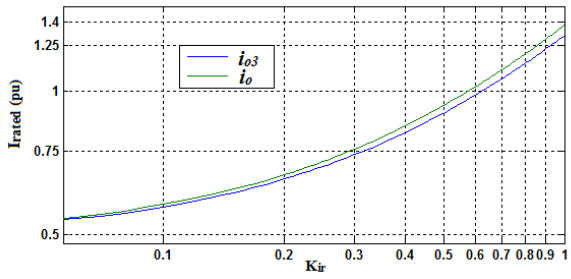

Fig. 12. Comparison between sinusoidal and third harmonic zero sequence injection with respect to estimated cluster current.

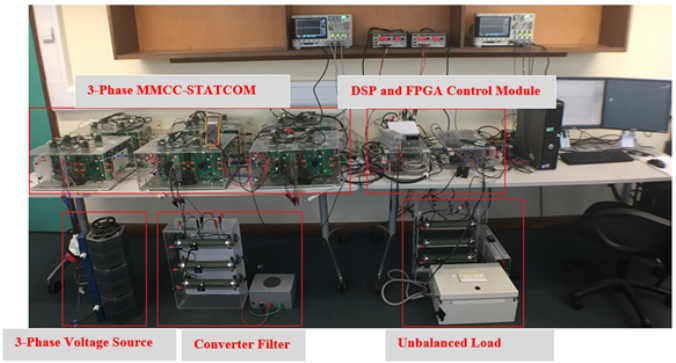

Fig. 13. Experimental MMCC STATCOM and associated system hardware.

converters as shown in Fig. 1(d). Hence there are six modules giving altogether 48 IGBT-diode switching pairs.

The parameters and component values of this experimental MMCC converter are given in Table 1. The switching scheme used is the multilevel phase-shifted PWM [35] with carrier frequency of $750Hz$. With two cascaded 3-level flying capacitor modules per phase, the effective lowest order harmonic frequency on the phase voltage is $(120\pm1)\times50Hz = (6000\pm50)Hz$. The filter parameters chosen are $1mH$, 1Ω which are effective in eliminating switching harmonics. The submodule capacitors were selected to ensure that their voltage ripples do not exceed $\pm10\%$ of its nominal voltage rating of $400V$. The principle of the design calculation is given in [36]. The controller gain parameters of the overall dc-link, cluster and circulating current $K_{p-dc} = 0.5$, $K_{i-dc} = 10$, $K_p = 1$, $K_i = 10$ and $K_{pio} = 30$ are selected to ensure zero steady state errors, less than 10% overshoots and fast transient responses.

The control scheme is implemented using a digital signal processor (DSP-TMS320C6713) which calculates the converter three-phase voltage reference values. For PWM signal generation a Field Programmable Gate Array (FPGA) (Actel ProAsic III) is used which is connected to the DSP external memory interface. Pulse signals are applied to the switches through fibre-optical cables.

For these tests the load was set to have a degree of load unbalance up to $K_{ir} = 0.7$. Figs. 14, 15 and 16 show the results obtained for the SSBC-MMCC, while results in Figs. 17, 18 and 19 are for the SDBC-MMCC. For each figure,

This article has been accepted for publication in a future issue of this journal, but has not been fully edited. Content may change prior to final publication. Citation information: DOI 10.1109/TIE.2018.2849962, IEEE Transactions on Industrial Electronics

the phase voltage and current waveforms are denoted as blue, green and red for phases a, b, c for star and ab, bc and ca for delta connections.

Fig. 14 shows the waveforms for the SSBC-based STATCOM for reactive power compensation under unbalanced load conditions while sinusoidal zero sequence voltage is injected. For comparison, Fig. 15 gives the corresponding waveforms under the same operating conditions but v_{o3} is injected for cluster dc-voltage balance. As can be seen from both figures, during the time interval $0 < t < 0.1sec$, the STATCOM operates under balanced load condition for reactive power compensation, so both v_o and v_{o3} are zero as shown in Fig. 14(f) and Fig. 15(f). The measured converter terminal voltages for SSBC converter under different K_{ir} values are shown in Fig. 16. When $K_{ir} = 0$, load current and terminal voltages are balanced as seen from Figs. 14(a), 15(a) and 16(a). From $t = 0.1sec$, load current imbalance occurs and the level of imbalance measured by K_{ir} increases from 0.21 to 0.65 in steps of 0.21, 0.105, 0.075 and 0.05 as shown in Fig. 14 for v_o injection. In Fig. 15, for v_{o3} injection, K_{ir} rises from 0.21 to 0.7 in steps of 0.21, 0.14, 0.09 and 0.05. The STATCOM controller compensates load unbalance in both cases.

It can be seen that when only injecting v_o, negative sequence current can be compensated for K_{ir} up to 0.6 ($0.1 < t < 0.5sec$) (see Fig. 14 (c)) and the dc-link capacitor voltages are maintained within their nominal ratings (see Fig. 14(e)). Fig. 16(b) shows the converter three terminal voltages when $K_{ir} = 0.42$, which are within the converter linear modulation range. However, further increasing the level of current imbalance to $K_{ir} = 0.65$ ($0.5 < t < 0.6sec$), the converter phase voltages, especially phase C voltage, rise fast hence exceeding the linear modulation range as seen in Fig. 14(c). This is due to high zero sequence voltage (reaching 60V) required as seen in Fig. 14(f). The dc-link capacitor voltages become uncontrollable because the phase limb voltages required to maintain the converter operation at $K_{ir} = 0.65$ are significantly over their limit (see Fig. 14(c)), thus resulting in distorted currents injecting into the grid as shown in Fig.14 (d). Fig. 16 (c) shows the converter terminal voltages at $K_{ir} = 0.65$ which are severely distorted and unbalanced.

In contrast, using the third harmonic zero sequence voltage v_{o3} injection, the operating range is extended as shown in Fig. 15. For $K_{ir} = 0.65$ within the time interval $0.4 < t < 0.5sec$, the converter reference and terminal voltages, particularly phase C voltage, are all still within the rated limit as seen in Fig. 15(c) and Fig. 16(d). Also, the dc-link voltage can be maintained balanced (see Fig. 15(e)). Thus it is clear that, using the third harmonic voltage injection technique, the SSBC-MMCC based STATCOM is able to operate normally for higher level of load current imbalance compared to the case when only fundamental zero sequence voltage v_o is used.

For comparison, the performance of the SDBC-MMCC based STATCOM under unbalanced load compensation is also investigated, and the results are as illustrated in Figs. 17 and 18. The superiority of the SDBC over the SSBC is mostly evident when the level of load imbalance is high. For example when $K_{ir} = 0.70$, the SDBC can compensate unbalanced current well, the sub-module capacitor voltages

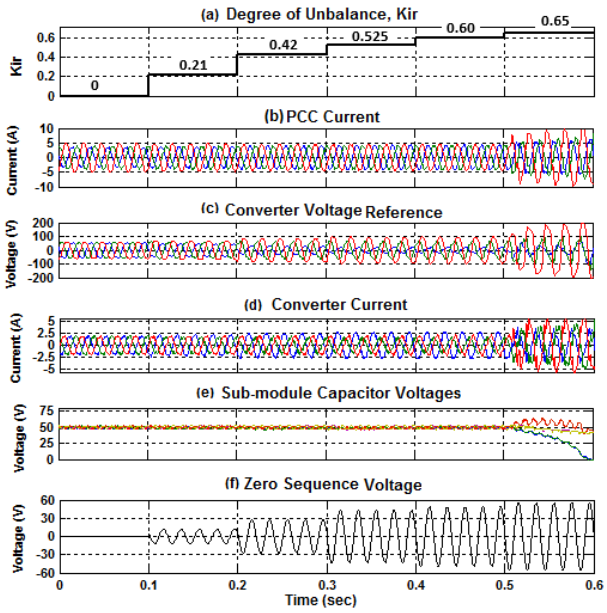

Fig. 14. Experimental results of SSBC-MMCC using v_o.

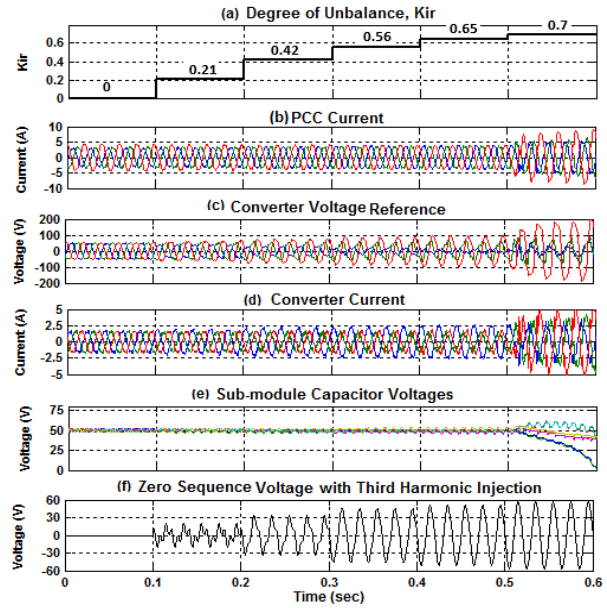

Fig. 15. Experimental results of SSBC-MMCC using v_{o3}.

are maintained within 10% of their nominal rated values (see Fig. 17(e) and 18(e)). In this case the results obtained from using zero sequence current i_o and third order harmonic plus fundamental zero sequence i_{o3} injections are also compared, the magnitude of i_{o3} required at $K_{ir} = 0.70$ is $0.1A$ lower than its counterpart which is $0.6A$ (see Fig. 17(f) and 18(f)). The converter terminal voltage waveforms are shown in Fig. 19 for K_{ir} equal to 0 and 0.70 respectively. From these waveforms, it is seen that for SDBC-MMCC, increase in the level of load imbalance does not result in large increment of the converter voltages.

This article has been accepted for publication in a future issue of this journal, but has not been fully edited. Content may change prior to final publication. Citation information: DOI 10.1109/TIE.2018.2849962, IEEE Transactions on Industrial Electronics

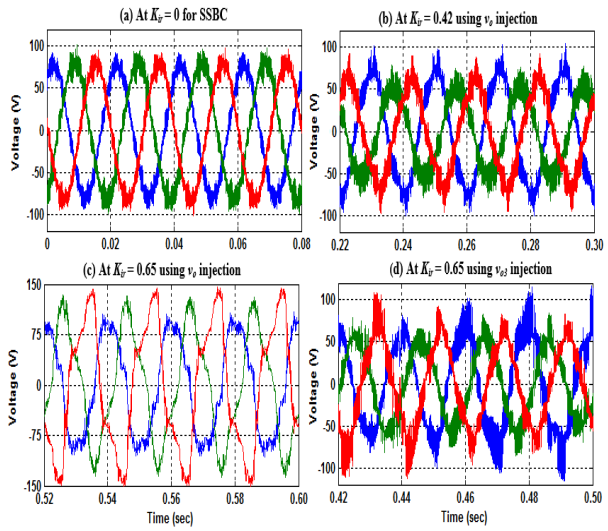

Fig. 16. SSBC converter terminal voltages at different K_{ir} values

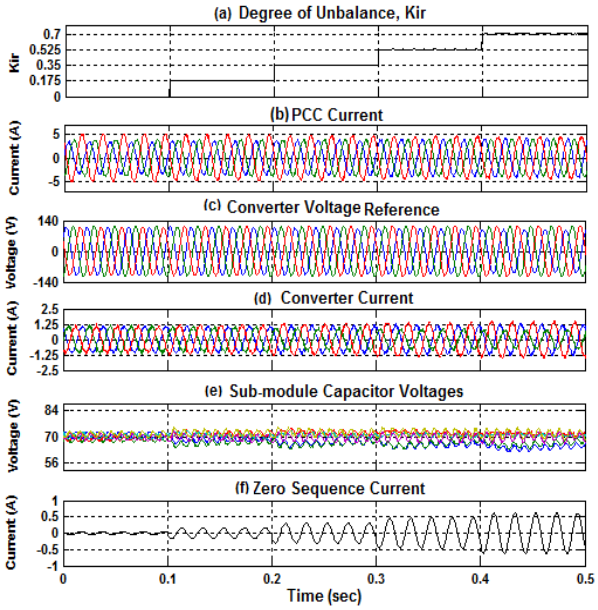

Fig. 17. Experimental results of SDBC-MMCC using i_o.

VI. Conclusion

This paper has proposed a new harmonic injection technique for star or delta configured MMCC-STATCOMs to balance their inter-cluster dc-link voltages when they are used for unbalanced load compensation. The theoretical and experimental contributions of this work can be summarized as follows:

1) Injecting a harmonic voltage for a star connected STATCOM reduces the maximum value of dc-link voltage, and injecting a harmonic current for a delta connected STATCOM reduces the maximum values of converter phase circulating current, compared to applying only sinusoidal zero sequence components, at a given degree of load unbalance.
2) This reduction improves the STATCOM capability for compensating unbalanced load current. Experimental results show that the SSBC-STATCOM is enabled to compensate unbalanced load up to 0.65, compared with the sinusoidal zero sequence voltage which can only cope with 0.60, while the converter phase cluster voltage for the latter is 12% higher.
3) Both SSBC and SDBC STATCOMs can compensate simultaneously the positive sequence reactive power and negative sequence active and reactive power. The SDBC-STATCOM is superior in unbalanced load compensation compared to its SSBC counterpart, and it can compensate up to 1.0 of load unbalance, K_{ir}.

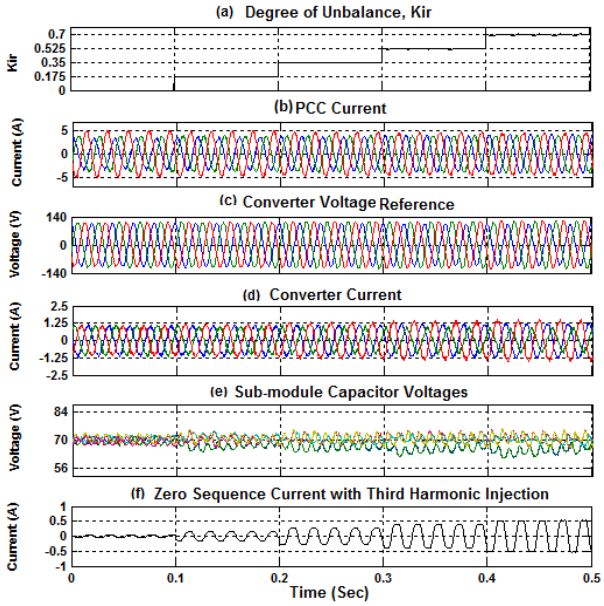

Fig. 18. Experimental results of SDBC-MMCC using i_{o3}.

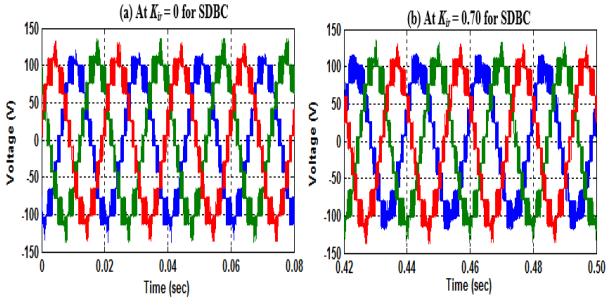

Fig. 19. SDBC converter terminal voltages at different K_{ir} values

References

[1] Mori S., Matsuno K., Hasegwa T., et al., *Development of a large static VAR generator using self-commutated inverters for improving power system.*, IEEE Trans. Power Systems, 1993, 8, (1), pp. 371-377.
[2] Nabae A, Takahashi I, Akagi H., et al., *A new neutral-point-clamped PWM inverter.*, IEEE Transactions on industry applications, 1981, (5), pp. 518-523.
[3] Meynard TA, Foch H., *Multi-level choppers for high voltage applications.*, EPE journal, 1992 Jan 1, 2(1), pp. 45-50.
[4] Kouro S, Malinowski M, Gopakumar K, et al., *Recent advances and industrial applications of multilevel converters.*, IEEE Transactions on industrial electronics, 2010 Aug; 57(8), pp. 2553-2580.

[5] Lai JS, Peng FZ., *Recent advances and industrial applications of multilevel converters.*, IEEE Transactions on industry applications, 1996 May; 32(3), pp. 509-517.

[6] Lesnicar A, Marquardt R., *A new modular voltage source inverter topology [C].*, In European Conference on Power Electronics and Applications (EPE), 2003.

[7] Akagi, Hirofumi., *Classification, terminology, and application of the modular multilevel cascade converter (MMCC).*, IEEE Transactions on Power Electronics 26.11 (2011): 3119-3130.

[8] Sano, Kenichiro, and Masahiro Takasaki., *A transformerless D-STATCOM based on a multivoltage cascade converter requiring no DC sources.*,IEEE transactions on power electronics 27.6 (2012): 2783-2795.

[9] Hagiwara, M., R. Maeda, and H. Akagi,*Application of a Modular Multilevel Cascade Converter (MMCC-SDBC) to a STATCOM.* IEEE Transactions on Industry Applications, 2011. 131: pp. 1433-1441.

[10] Nwobu, C., Oghorada,O.J.K., et al., *A modular multilevel flying capacitor converter-based STATCOM for reactive power control in distribution systems.* in Power Electronics and Applications (EPE'15), 17th European Conference on. 2015.

[11] Gultekin, Burhan, and Muammer Ermis., *Cascaded multilevel converter-based transmission STATCOM: System design methodology and development of a 12 kV $\pm$12 MVAr power stage.*,IEEE transactions on power electronics 28.11 (2013): 4930-4950.

[12] H. Akagi, S. Inoue, and T. Yoshii, *Control and performance of a transformerless cascade PWM STATCOM with star configuration.*,IEEE transactions on Industry Applications, vol. 43, no. 4, pp. 1041-1049, 2007.

[13] W. Ping-Heng, C. Hsin-Chih, et al., *Delta-connected cascaded H-bridge converter application in unbalanced load compensation.*,IEEE Transactions on Industry Applications 53, no. 2 (2017): 1254-1262.

[14] Y. Shi, B. Liu, Y. Shi, and S. Duan, *Individual Phase Current Control Based on Optimal Zero-Sequence Current Separation for a Star-Connected Cascade STATCOM Under Unbalanced Conditions.*,IEEE Transactions on Power Electronics, 2016, vol. 31, no. 3, pp. 2099-2110.

[15] Sixing, D. and L. Jinjun, *A Study on DC Voltage Control for Chopper-Cell-Based Modular Multilevel Converters in D-STATCOM Application.* Power Delivery, IEEE Transactions on, 2013. 28(4): p. 2030-2038.

[16] M. Nieves, J. M. Maza, J. M. Mauricio, R. Teodorescu, M. Bongiorno, and P. Rodriguez, *Enhanced control strategy for MMC-based STATCOM for unbalanced load compensation.* In Power Electronics and Applications (EPE'14-ECCE Europe), 16th European Conference on, pp. 1-10. IEEE, 2014.

[17] S. Qiang, and L. Wenhua, *Control of a Cascade STATCOM With Star Configuration Under Unbalanced Conditions,* IEEE Transactions on Power Electronics, vol. 24, no. 1, pp. 45-58, 2009.

[18] O. J. K. Oghorada, and L. Zhang, *Analysis of star and delta connected modular multilevel cascaded converter-based STATCOM for load unbalanced compensation.* International Journal of Electrical Power & Energy Systems, vol. 95, pp. 341-352, 2018.

[19] Behrouzian, E. and M. Bongiorno, *Investigation of Negative-Sequence Injection Capability of Cascaded H-Bridge Converters in Star and Delta Configuration.* IEEE Transactions on Power Electronics, 2016. (99): p. 1-6.

[20] X. She, A. Q. Huang, and G. Wang, *3-D Space Modulation With Voltage Balancing Capability for a Cascaded Seven-Level Converter in a Solid-State Transformer.* IEEE Transactions on Power Electronics,vol. 26, no. 12, pp. 3778-3789, 2011.

[21] Y. Zhang, G. P. Adam, T. C. Lim, S. J. Finney, and B. W. Williams, *Hybrid Multilevel Converter: Capacitor Voltage Balancing Limits and its Extension.* IEEE Transactions on Industrial Informatics, vol. 9, no. 4, pp. 2063-2073, 2013.

[22] Summers, T.J., R.E. Betz, and G. Mirzaeva. *Phase leg voltage balancing of a cascaded H-Bridge converter based STATCOM using zero sequence injection.* in Power Electronics and Applications, 2009. EPE '09. 13th European Conference on. 2009.

[23] Ota, João I. Yutaka, Yuji Shibano, and Hirofumi Akagi. *A phase-shifted PWM D-STATCOM using a modular multilevel cascade converter (SSBC)Part II: Zero-voltage-ride-through capability.*IEEE Transactions on Industry Applications, 51(1), (2015), pp. 289-296.

[24] O.J.K. Oghorada, C. Nwobu, and L. Zhang, *Control of a Single-Star Flying Capacitor Converter Modular Multi-level Cascaded Converter*

[25] Sochor, P. and H. Akagi, *Theoretical Comparison in Energy-Balancing Capability Between Star- and Delta-Configured Modular Multilevel Cascade Inverters for Utility-Scale Photovoltaic Systems.* Power Electronics, IEEE Transactions on, 2016. 31(3): pp. 1980-1992.

(SSFCC-MMCC) STATCOM for Unbalanced Load Compensation.,8th IET International Conference on Power Electronics, Machines and Drives, 2016.

[26] Y. Yu, V. G. Agelidis, et al, *Comparison of zero-sequence injection methods in cascaded H-bridge multilevel converters for large-scale photovoltaic integration,* IET Renewable Power Generation, vol. 11, no. 5, pp. 603-613, 2016.

[27] Yifan, Y., G., Konstantinou, B., Hredzak and V.G., Agelidis, *Power Balance Optimization of Cascaded H-Bridge Multilevel Converters for Large-Scale Photovoltaic Integration.* , IEEE Transactions on Power Electronics, 2016. 31(2): p. 1108-1120.

[28] X. Bailu, H. Lijun, M. Jun, C. Riley, L. M. Tolbert, and B. Ozpineci, *Modular Cascaded H-Bridge Multilevel PV Inverter With Distributed MPPT for Grid-Connected Applications,* IEEE Transactions on Industry Applications, vol. 51, no. 2, pp. 1722-1731, 2015.

[29] Hatano, Nobuhiko, and Toshifumi Ise. *Control scheme of cascaded H-bridge STATCOM using zero-sequence voltage and negative-sequence current.*,IEEE Transactions on Power Delivery 25.2 (2010): 543-550.

[30] S. Bifaretti, A. Lidozzi, L. Solero, and F. Crescimbini, *Modulation with sinusoidal third-harmonic injection for active split DC-bus four-leg inverters.*,IEEE Transactions on Power Electronics, vol. 31, no. 9, (2016): 6226-6236.

[31] Wang H, Su M, Sun Y, et al., *Active third-harmonic injection indirect matrix converter with dual three-phase outputs.*,IET Power Electronics, 2016 Mar 30; 9(4):657-668.

[32] Guo G, Song Q, Yang W, et al., *Application of Third-Order Harmonic Voltage Injection in a Modular Multilevel Converter.*,IEEE Transactions on Industrial Electronics, 2018 Jul;65(7):5260-5271.

[33] Holmes, D.G. and T.A. Lipo, *Pulse width modulation for power converters: principles and practice.* Vol. 18. 2003: John Wiley & Sons.

[34] Akagi, H., E.H. Watanabe, and M. Aredes, *Instantaneous power theory and applications to power conditioning.* Vol. 31. 2007: John Wiley & Sons.

[35] Oghorada, O. J. K., and Li Zhang. *Control of a Modular Multi-level Converter STATCOM for low voltage ride-through condition.* Industrial Electronics Society, IECON 2016-42nd Annual Conference of the IEEE. IEEE, 2016.

[36] Oghorada, O. J. K., *Modular Multilevel Cascaded Flying Capacitor STATCOM for Balanced and Unbalanced load Compensation,* PhD., School of Electronic/Electrical Engineering, University of Leeds, 2017.

O ghenewvogaga Oghorada (M'13) was born in Ughelli, Delta state, Nigeria in 1987 and received B.Eng. degree in Electrical Engineering from Igbinedion University, Okada, Edo state, Nigeria in 2009. He received M.Sc. and PhD degrees in Electronic/Electrical Engineering from University of Leeds, United Kingdom in 2012 and 2017 respectively.

He is currently a lecturer at the department of Electrical and Information Engineering, Landmark University, Omu-aran, Kwara state, Nigeria. His research interests include modulation and control of power converters, multilevel converters, modular multilevel converters, FACTs devices, HVDC transmission systems, Renewable energy systems and Energy management.

L i Zhang (M'80) received PhD degree in 1985 from Bradford University in UK in 1985. She has been a research associate in Oxford University, UK and a lecturer and now associate professor in the School of Electronics and Electrical Engineering in the University of Leeds.UK.

She became a Visiting Professor with ChongQing University, China, in 2006. She is the associate editor for IEEE Transactions on Power Electronics and has also been the associate editor for IET Proceedings on Power Electronics 2014-2017.

Her current research interests are in power electronic converters and applications for power systems, FACTS devices and renewable sourced generators.